Footprints of New Physics in $b \to c\tau\nu$ Transitions

Zhuoran Huang

Institute of High Energy Physics, CAS

huangzr@ihep.ac.cn

December 20, 2018

Outline

Experimental Status

- The combined results of $R(D)$ and $R(D^*)$ measured by BABAR, BELLE and LHCb are $R(D) = 0.407 \pm 0.024$ and $R(D^*) = 0.304 \pm 0.013 \pm 0.007$, which clearly indicates the deviation from the SM predictions by 2.3σ and 3.4σ respectively.

$$R(D^{(*)}) = \frac{\mathcal{B}(B \to D^{(*)}\tau\nu)}{\mathcal{B}(B \to D^{(*)}\ell\nu)}, \qquad \text{with } \ell = \mu, e.$$

- Most recently LHCb reported the ratio

$$R(J/\psi) = \frac{\mathcal{B}(B_c \to J/\psi\tau\nu)}{\mathcal{B}(B_c \to J/\psi\mu\nu)} = 0.71 \pm 0.17 \pm 0.18.$$

This result deviates 2σ away from the SM predictions.

Theoretical Formalism

- The basic starting point for doing phenomenology in weak decays of hadrons is the weak effective Hamiltonian

$$H_{eff} = \frac{G_F}{\sqrt{2}} \sum_i V_{CKM}^i C_i(\mu) O_i$$

- For the $b \to c\tau\nu$ transitions, the four-fermion operator basis can be defined as

$$\mathcal{O}_{S_1} = (\overline{c}_L b_R)(\overline{\tau}_R \nu_L)\,, \quad \mathcal{O}_{S_2} = (\overline{c}_R b_L)(\overline{\tau}_R \nu_L)\,,$$
$$\mathcal{O}_{V_1} = (\overline{c}_L \gamma^\mu b_L)(\overline{\tau}_L \gamma_\mu \nu_L)\,, \quad \mathcal{O}_{V_2} = (\overline{c}_R \gamma^\mu b_R)(\overline{\tau}_L \gamma_\mu \nu_L)\,,$$
$$\mathcal{O}_T = (\overline{c}_R \sigma^{\mu\nu} b_L)(\overline{\tau}_R \sigma_{\mu\nu} \nu_L)\,.$$

$B \to D^{(*)}$ Form Factors in HQET

F. U. Bernlochner, Z. Ligeti, M. Papucci and D. J. Robinson, Phys. Rev. D **95**, *no. 11, 115008 (2017)*

$$
\begin{aligned}
\langle D(k)|\bar{c}\gamma^\mu b|\overline{B}(p)\rangle &= \sqrt{m_B m_D}\left[h_+(w)(v+v')^\mu + h_-(w)(v-v')^\mu\right] \\
\langle D(k)|\bar{c}b|\bar{B}(p)\rangle &= \sqrt{m_B m_D}(w+1)h_S(w)\,, \\
\langle D(k)|\bar{c}\sigma^{\mu\nu}b|\bar{B}(p)\rangle &= -i\sqrt{m_B m_D}h_T(w)(v^\mu v'^\nu - v^\nu v'^\mu)\,, \\
\langle D^*(k,\epsilon)|\bar{c}\gamma^\mu b|\bar{B}(p)\rangle &= i\sqrt{m_B m_{D^*}}\,h_V(w)\varepsilon^{\mu\nu\rho\sigma}\epsilon^*_\nu v'_\rho v_\sigma\,, \\
\langle D^*(k,\epsilon)|\bar{c}\gamma^\mu\gamma^5 b|\bar{B}(p)\rangle &= \sqrt{m_B m_{D^*}}\left[h_{A_1}(w)(w+1)\epsilon^{*\mu}\right. \\
&\quad \left.-(\epsilon^*\cdot v)\left(h_{A_2}(w)v^\mu + h_{A_3}(w)v'^\mu\right)\right], \\
\langle D^*(k,\epsilon)|\bar{c}\gamma^5 b|\bar{B}(p)\rangle &= -\sqrt{m_B m_{D^*}}\,(\epsilon^*\cdot v)h_P(w), \\
\langle D^*(k,\epsilon)|\bar{c}\sigma^{\mu\nu}b|\bar{B}(p)\rangle &= -\sqrt{m_B m_{D^*}}\,\varepsilon^{\mu\nu\rho\sigma}\Big[h_{T_1}(w)\epsilon^*_\rho(v+v')_\sigma + h_{T_2}(w) \\
&\quad +h_{T_3}(w)(\epsilon^*\cdot v)v_\rho v'_\sigma\Big]\,,
\end{aligned}
$$

where the dimensionless kinematic variable $w = v\cdot v' = \frac{m_B^2+m_D^2-(p_B-p_D)^2}{2m_B m_D}$ is used instead of the momentum transfer $q^2 = (p-k)^2$.

In the heavy quark limit, only the single leading Isgur-Wise function $\xi(w)$ is needed for expressing the $B \to D^{(*)}$ form factors. With inclusion of the $\mathcal{O}(\alpha_s, \Lambda_{\rm QCD}/m_{b,c})$ contributions, these form factors are written as

$$
\begin{aligned}
h_+ &= \xi\left\{1 + \hat{\alpha}_s\left[C_{V_1} + \frac{w+1}{2}\left(C_{V_2} + C_{V_3}\right)\right] + \left(\varepsilon_c + \varepsilon_b\right)\hat{L}_1\right\}, \\
h_- &= \xi\left[\hat{\alpha}_s\,\frac{w+1}{2}\left(C_{V_2} - C_{V_3}\right) + \left(\varepsilon_c - \varepsilon_b\right)\hat{L}_4\right], \\
h_S &= \xi\left[1 + \hat{\alpha}_s\, C_S + \left(\varepsilon_c + \varepsilon_b\right)\left(\hat{L}_1 - \hat{L}_4\,\frac{w-1}{w+1}\right)\right], \\
h_T &= \xi\left[1 + \hat{\alpha}_s\left(C_{T_1} - C_{T_2} + C_{T_3}\right) + \left(\varepsilon_c + \varepsilon_b\right)\left(\hat{L}_1 - \hat{L}_4\right)\right], \\
&\cdots
\end{aligned}
$$

The $L_{1\ldots6}$ functions can be expressed in terms of the sub-leading Isgur-Wise functions through:

$$\hat{L}_1 = -4(w-1)\hat{\chi}_2 + 12\hat{\chi}_3\,, \qquad \hat{L}_2 = -4\hat{\chi}_3\,, \qquad \hat{L}_3 = 4\hat{\chi}_2\,,$$
$$\hat{L}_4 = 2\eta - 1\,, \qquad \hat{L}_5 = -1\,, \qquad \hat{L}_6 = -2(1+\eta)/(w+1)\,.$$

With $\hat{\chi}_3(1) = 0$ implied by the Luke's theorem, up to $\mathcal{O}(\varepsilon_{c,b}(w-1))$ the subleading Isgur-Wise functions can be approximated as follows:

$$\hat{\chi}_2(w) \simeq \hat{\chi}_2(1) + \hat{\chi}_2'(1)(w-1)\,, \quad \hat{\chi}_3(w) \simeq \hat{\chi}_3'(1)(w-1)\,,$$
$$\eta(w) \simeq \eta(1) + \eta'(1)(w-1)\,.$$

Global Fit of the HQET Parameters

M. Jung and D. M. Straub, arXiv:1801.01112

- Lattice QCD at zero hadronic recoil
- Light-cone sum rule at large hadronic recoil
- Strong unitarity constraints
- 1S Scheme (ensuring the renormalon cancellation)

$$\begin{pmatrix} \chi_2(1) \\ \chi_2'(1) \\ \chi_3'(1) \\ \eta(1) \\ \eta'(1) \\ \rho^2 \\ c \\ \delta_{h_{A_1}} \\ \delta_{h_+} \end{pmatrix} = \begin{pmatrix} -0.058 \pm 0.019 \\ -0.001 \pm 0.020 \\ 0.035 \pm 0.019 \\ 0.358 \pm 0.043 \\ 0.044 \pm 0.125 \\ 1.306 \pm 0.059 \\ 1.220 \pm 0.109 \\ -2.299 \pm 0.394 \\ 0.485 \pm 0.269 \end{pmatrix},$$

$$
\begin{pmatrix}
1.00 & 0.01 & 0.02 & -0.00 & 0.02 & -0.27 & -0.21 & -0.03 & 0.02 \\
0.01 & 1.00 & -0.00 & -0.02 & -0.02 & 0.00 & 0.14 & 0.01 & 0.00 \\
0.02 & -0.00 & 1.00 & 0.00 & -0.03 & 0.83 & 0.61 & -0.03 & 0.02 \\
-0.00 & -0.02 & 0.00 & 1.00 & 0.03 & 0.01 & 0.04 & 0.15 & 0.21 \\
0.02 & -0.02 & -0.03 & 0.03 & 1.00 & -0.14 & -0.16 & -0.05 & -0.22 \\
-0.27 & 0.00 & 0.83 & 0.01 & -0.14 & 1.00 & 0.79 & 0.09 & -0.14 \\
-0.21 & 0.14 & 0.61 & 0.04 & -0.16 & 0.79 & 1.00 & 0.06 & -0.08 \\
-0.03 & 0.01 & -0.03 & 0.15 & -0.05 & 0.09 & 0.06 & 1.00 & -0.24 \\
0.02 & 0.00 & 0.02 & 0.21 & -0.22 & -0.14 & -0.08 & -0.24 & 1.00
\end{pmatrix}
$$

$B_c \to J/\psi(\eta_c)$ Form Factors

$$\langle \eta_c(k)|\bar{c}\gamma_\mu b|B_c(p)\rangle = \left[(p+k)_\mu - \frac{m^2_{B_c} - m^2_{\eta_c}}{q^2} q_\mu\right] F_1(q^2) + q_\mu \frac{m^2_{B_c} - m^2_{\eta_c}}{q^2} F_0(q^2)\,,$$

$$\langle J/\psi(k)|\bar{c}\gamma^\mu b|B_c(p)\rangle = -\frac{2iV(q^2)}{m_{B_c} + m_{J/\psi}} \varepsilon^{\mu\nu\rho\sigma} \epsilon^*_\nu p_\rho k_\sigma\,,$$

$$\begin{aligned}\langle J/\psi(k)|\bar{c}\gamma^\mu\gamma^5 b|B_c(p)\rangle = {} & 2m_{J/\psi} A_0(q^2) \frac{\epsilon^* \cdot q}{q^2} q^\mu + (m_{B_c} + m_{J/\psi}) A_1(q^2) \left[\epsilon^{*\mu} - \frac{\epsilon^* \cdot q}{q^2} q^\mu\right] \\ & - A_2(q^2) \frac{\epsilon^* \cdot q}{m_{B_c} + m_{J/\psi}} \left[p^\mu + k^\mu - \frac{m^2_{B_c} - m^2_{J/\psi}}{q^2} q^\mu\right],\end{aligned}$$

where the form factors are parametrized as $F(q^2) = F(0)\,\exp(c_1\hat{s} + c_2\hat{s}^2)$ with $\hat{s} = q^2/m^2_{B_c}$ in the full kinematical range of q^2, of which the results computed in the covariant light-front quark model.

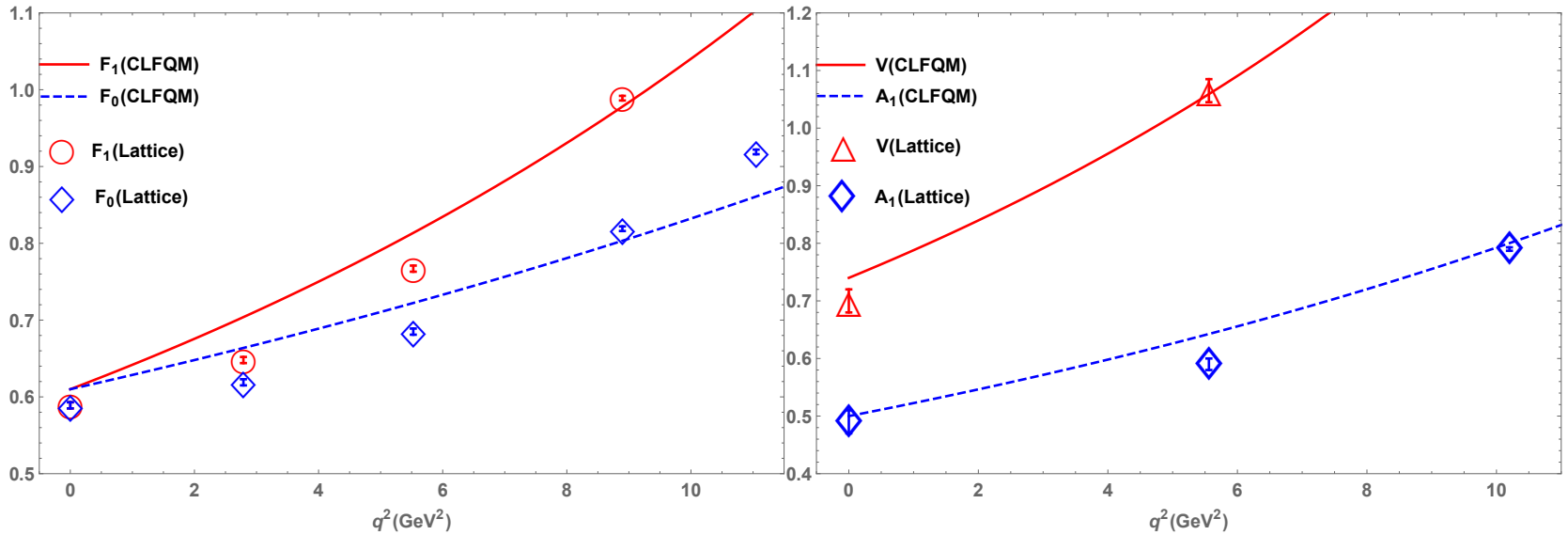

Figure: CLFQM form factors for the $B_c \to \eta_c$ and $B_c \to J/\psi$ hadronic transitions in comparison with the preliminary lattice results.

W. Wang, Y. L. Shen and C. D. Lu, Phys. Rev. D **79**, *054012 (2009)*
B. Colquhoun et al. [HPQCD Collaboration], PoS LATTICE **2016**, *281 (2016)*

$T(q^2)$ have not been calculated in CLFQM but can be related to $V(q^2)$ and $A(q^2)$ through the quark level equations of motion:

$$F_T(q^2) = -\frac{(m_b + m_c)}{q^2}(m_{B_c} + m_{\eta_c})\big(F_0(q^2) - F_1(q^2)\big)\,,$$

$$T_1(q^2) = \frac{m_b + m_c}{m_{B_c} + m_{J/\psi}} V(q^2)\,,$$

$$T_2(q^2) = \frac{m_b - m_c}{m_{B_c} - m_{J/\psi}} A_1(q^2)\,,$$

$$T_3(q^2) = -\frac{m_b - m_c}{q^2}\Big[m_{B_c}\big(A_1(q^2) - A_2(q^2)\big) + m_{J/\psi}\big(A_2(q^2) + A_1(q^2) - 2A_0(q^2)\big)\Big]\,,$$

where we use the quark masses in the $\overline{MS}$ renormalization scheme at the scale $\mu = \overline{m}_b$ and to be more conservative consider the differences in the numerical results induced by using the pole quark masses as a source of systematic uncertainties.

χ^2 Fit of the Wilson Coefficients

χ^2 as a function of the Wilson coefficient C_X:

$$\chi^2(C_X) = \sum_{m,n=1}^{\text{data}} (O^{th}(C_X) - O^{exp})_m (V^{exp} + V^{th})^{-1}_{mn} (O^{th}(C_X) - O^{exp})_n + \frac{(R^{th}_{J/\psi}(C_X) - R^{exp}_{J/\psi})^2}{\sigma^2_{R_{J/\psi}}},$$

Table: Experimental data used in the fit.

	R_D	R_{D^*}	Correlation	$P_\tau(D^*)$	$R_{J/\psi}$
BABAR, 12	0.440(58)(42)	0.332(24)(18)	−0.27	–	–
Belle, 15	0.375(64)(26)	0.293(38)(15)	−0.49	–	–
Belle, 16	–	0.302(30)(11)	–	–	–
Belle, 17	–	$0.270(35)(^{+0.028}_{-0.025})$	0.33	$-0.38(51)(^{+0.21}_{-0.16})$	–
LHCb, 15	–	0.336(27)(30)	–	–	–
LHCb, 18	–	0.291(19)(26)(13)	–	–	–
LHCb, 18	–	–	–	–	0.71(17)(18)

Table: Fitted values of the Wilson coefficients in different NP scenarios.

NP scenario	value	χ^2/dof	Correlation
C_{V_1}	$(1+Re[C_{V_1}])^2+(Im[C_{V_1}])^2=1.27(6)$	7.42/8	–
C_{V_2}	$0.057(50)\pm 0.573(73)i$	6.19/8	0.750
C_{S_1}	0.405(91)	15.5/8	–
C_{S_2}	$-1.05(30)\pm 1.09(12)i$	5.98/8	0.589
C_T	$0.24(11)\pm 0.13(8)i$	8.39/8	−0.993

1σ Constraints on the NP Scenarios

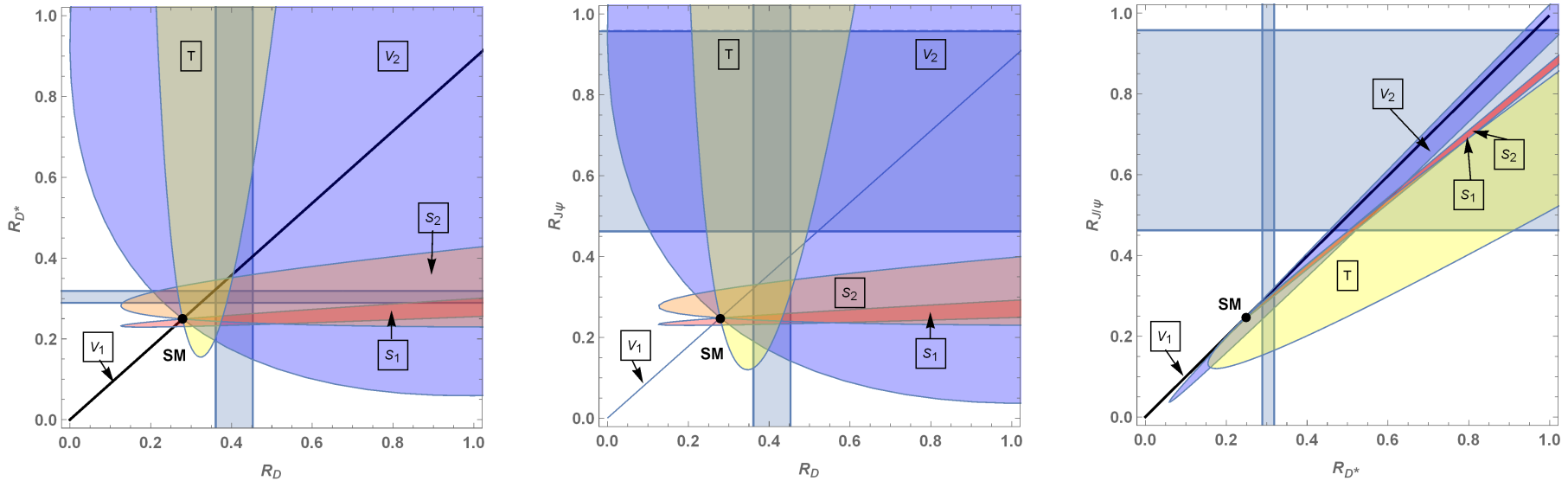

Figure: Correlations between $R(D)$, $R(D^*)$ and $R(J/\psi)$ in the presence of single NP operators. The vertical and horizontal bands show the experimental constraints and the black dots denote the SM predictions.

2σ Constraints on the NP Wilson coefficients

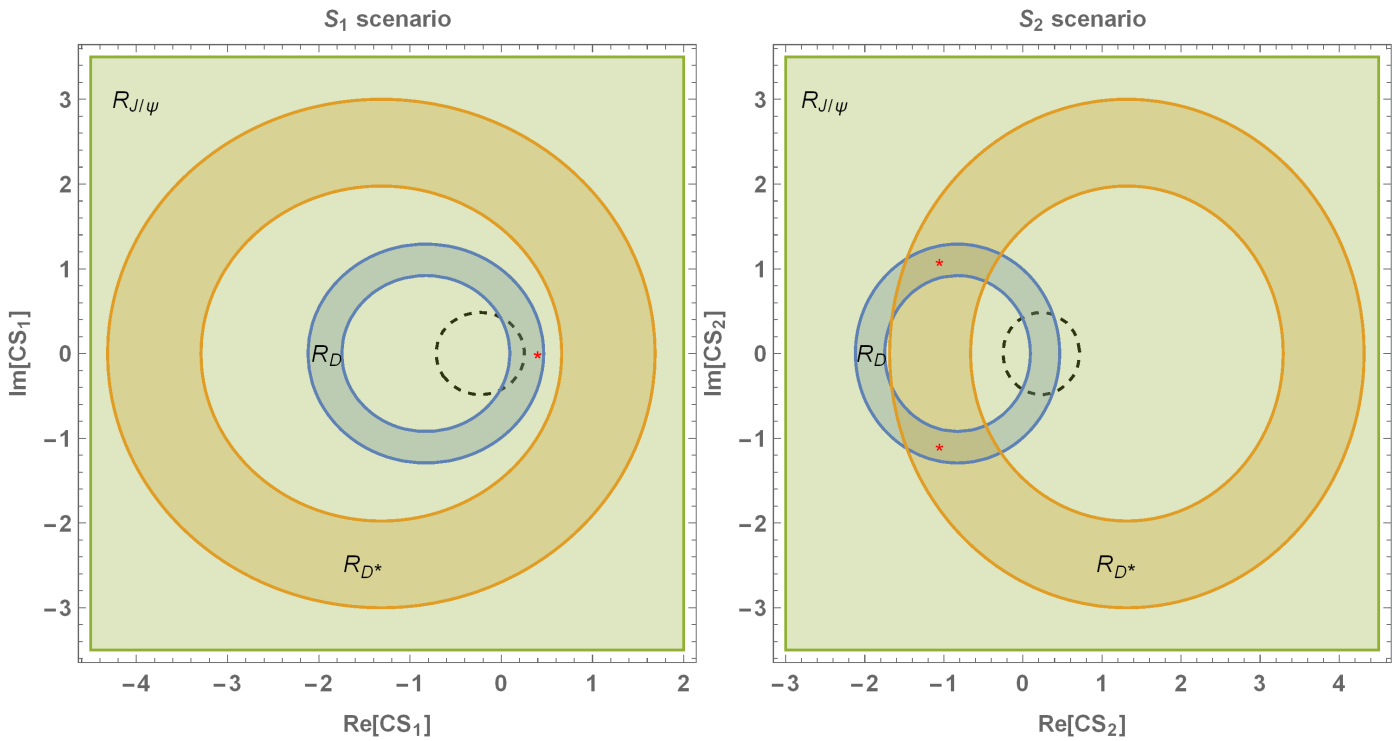

Figure: Constraints on the Wilson coefficients from the measurements of $R(D^{(*)})$ and $R(J/\psi)$ at the C.L. of 2σ and the branching fraction $\mathcal{B}(B_c \to \tau\nu)$ (black dashed curves). In each panel the red stars or dashed curves denote the optimal values obtained by using the fitted Wilson coefficients.

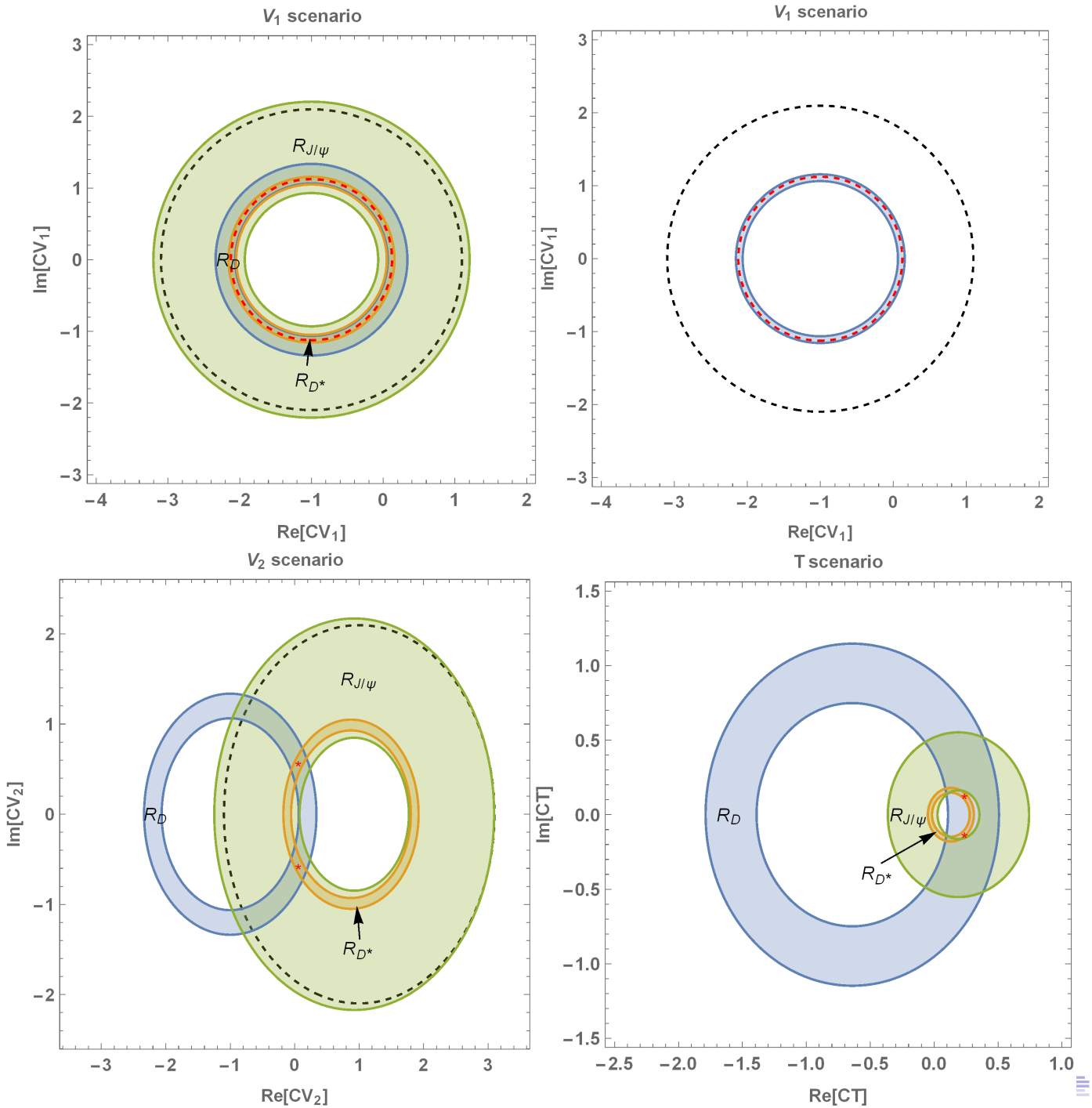
V_1 scenario
$R_{J/\psi}$
R_D
R_{D^*}
Im[CV_1]
Re[CV_1]
V_1 scenario
Im[CV_1]
Re[CV_1]
V_2 scenario
$R_{J/\psi}$
R_D
R_{D^*}
Im[CV_2]
Re[CV_2]
T scenario
R_D
$R_{J/\psi}$
R_{D^*}
Im[CT]
Re[CT]

Predictions for the Observables

Table: Predictions for observables involved in the $B \to D^{(*)}$ decays. The first and second uncertainties respectively result from the input parameters and the fitted Wilson coefficients.

Scenario	$R(D)$	$R(D^*)$	$P_\tau(D)$	$P_\tau(D^*)$	P_{D^*}	$\mathcal{A}_{FB}(D)$
SM	0.279(7)(0)	0.249(4)(0)	0.325(3)(0)	−0.508(4)(0)	0.441(6)(0)	0.3606(6)(0)
V_1	0.354(9)(19)	0.317(5)(17)	0.325(3)(0)	−0.508(4)(0)	0.441(6)(0)	0.3606(6)(0)
V_2	0.403(10)(48)	0.307(5)(15)	0.325(3)(0)	−0.509(4)(1)	0.436(7)(4)	0.3606(6)(0)
T	0.371(10)(42)	0.313(26)(15)	0.180(5)(49)	0.038(1)(118)	0.173(11)(60)	0.4311(5)(29)

Table: Predicted ranges for observables involved in the $B \to D^{(*)}$ decays from the experimental constraints within 2σ and the limit of $\mathcal{B}(B_c \to \tau\nu)$.

Senario	$R(D)$	$R(D^*)$	$P_\tau(D)$	$P_\tau(D^*)$	P_{D^*}	$\mathcal{A}_{FB}(D)$
V_1	[0.315, 0.373]	[0.282, 0.334]	[0.325, 0.325]	[−0.508, −0.508]	[0.441, 0.441]	[0.361, 0.361]
V_2	[0.315, 0.499]	[0.274, 0.334]	[0.325, 0.325]	[−0.511, −0.508]	[0.429, 0.441]	[0.361, 0.361]
T	[0.321,0.323]	[0.274, 0.334]	[0.248, 0.249]	[−0.234, −0.182]	[0.287, 0.306]	[0.395, 0.398]

Table: Predictions for observables involved in the $B_c \to \eta_c(J/\psi)$ decays. The first, second and third uncertainties respectively result from the input parameters, the fitted Wilson coefficients and the quark mass schemes for the tensor form factors.

Scenario	$R(\eta_c)$	$R(J/\psi)$	$P_\tau(J/\psi)$
SM	$0.281(^{+0.034}_{-0.030})(0)$	$0.248(6)(0)$	$-0.512(^{+0.021}_{-0.016})(0)$
V_1	$0.357(^{+0.044}_{-0.038})(19)$	$0.315(7)(17)$	$-0.512(^{+0.021}_{-0.016})(0)$
V_2	$0.406(^{+0.050}_{-0.044})(49)$	$0.304(7)(16)$	$-0.512(^{+0.021}_{-0.016})(1)$
T	$0.337(^{+0.019}_{-0.015})(26)(15)$	$0.188(^{+0.017}_{-0.012})(10)(21)$	$-0.028(^{+0.016}_{-0.013})(175)(53)$

$P_\tau(\eta_c)$	$P_{J/\psi}$	$\mathcal{A}_{FB}(\eta_c)$	$\mathcal{A}_{FB}(J/\psi)$
$0.347(81)(0)$	$0.446(6)(0)$	$0.364(^{+0.007}_{-0.009})(0)$	$-0.042(11)(0)$
$0.347(81)(0)$	$0.446(6)(0)$	$0.364(^{+0.007}_{-0.009})(0)$	$-0.042(11)(0)$
$0.347(81)(0)$	$0.443(6)(3)$	$0.364(^{+0.007}_{-0.009})(0)$	$0.031(7)(13)$
$0.24(^{+0.15}_{-0.13})(4)(2)$	$0.271(14)(64)(41)$	$0.419(^{+0.014}_{-0.031})(23)(8)$	$-0.036(^{+0.010}_{-0.008})(49)(21)$

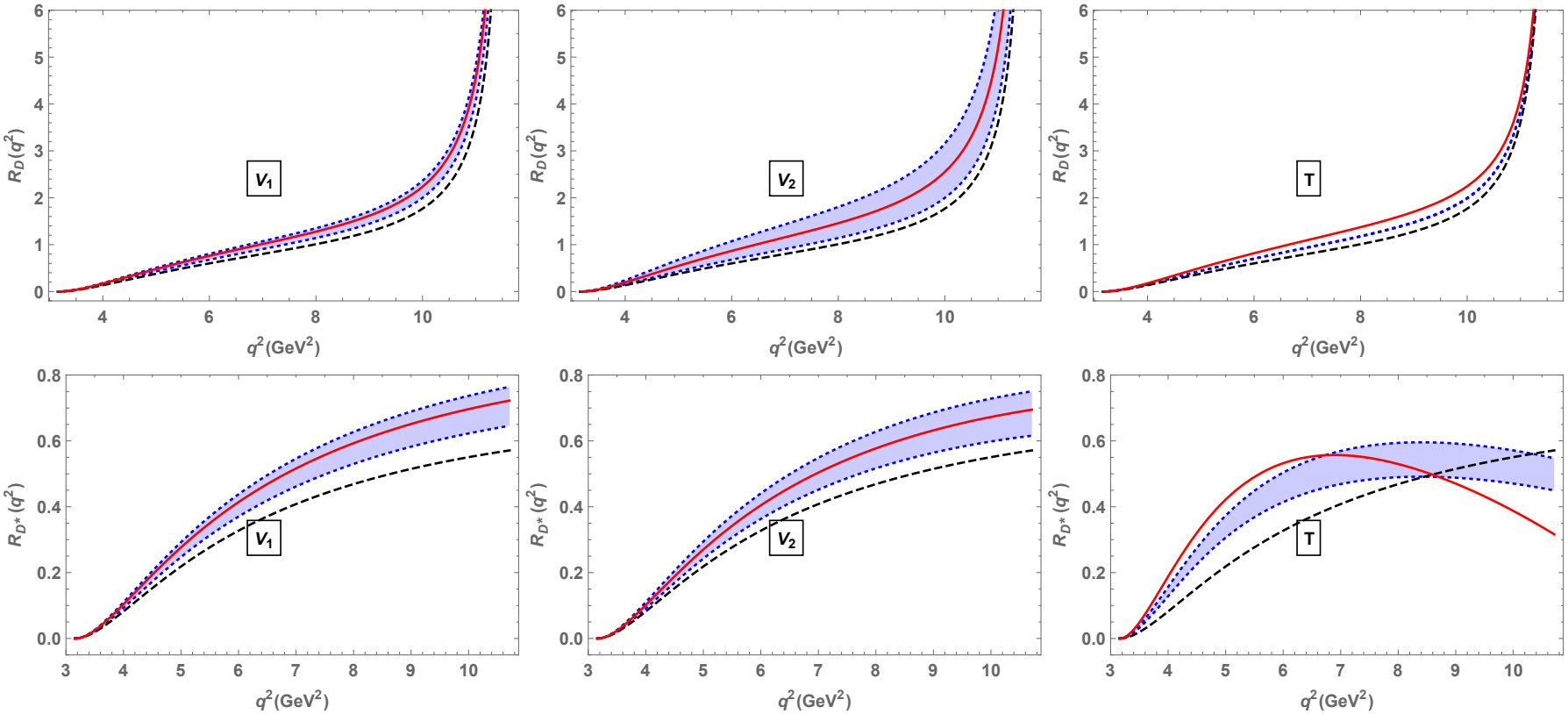

Figure: Predictions for the differential ratios $R_D(q^2)$ and $R_{D*}(q^2)$. The black dashed lines and the red solid lines respectively denote the SM predictions and the NP predictions corresponding to the best fitted Wilson coefficients. The light blue bands include NP effects corresponding to the experimental constraints within 2σ.

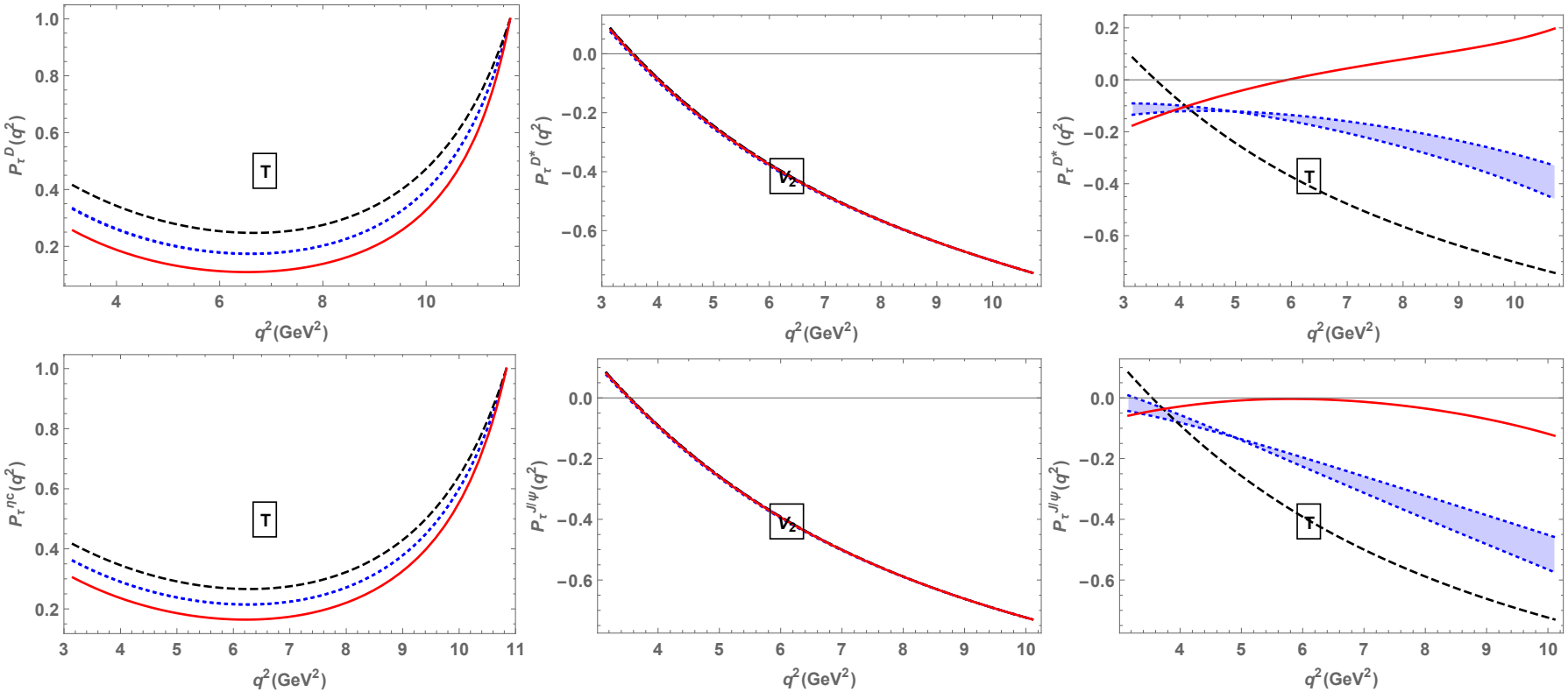

Figure: Predictions for the differential polarizations $P_\tau^{D^{(*)}}(q^2)$, $P_\tau^{\eta_c}(q^2)$ and $P_\tau^{J/\psi}(q^2)$. The black dashed lines and the red solid lines respectively denote the SM predictions and the NP predictions corresponding to the best fitted Wilson coefficients. The light blue bands include NP effects corresponding to the experimental constraints within 2σ.

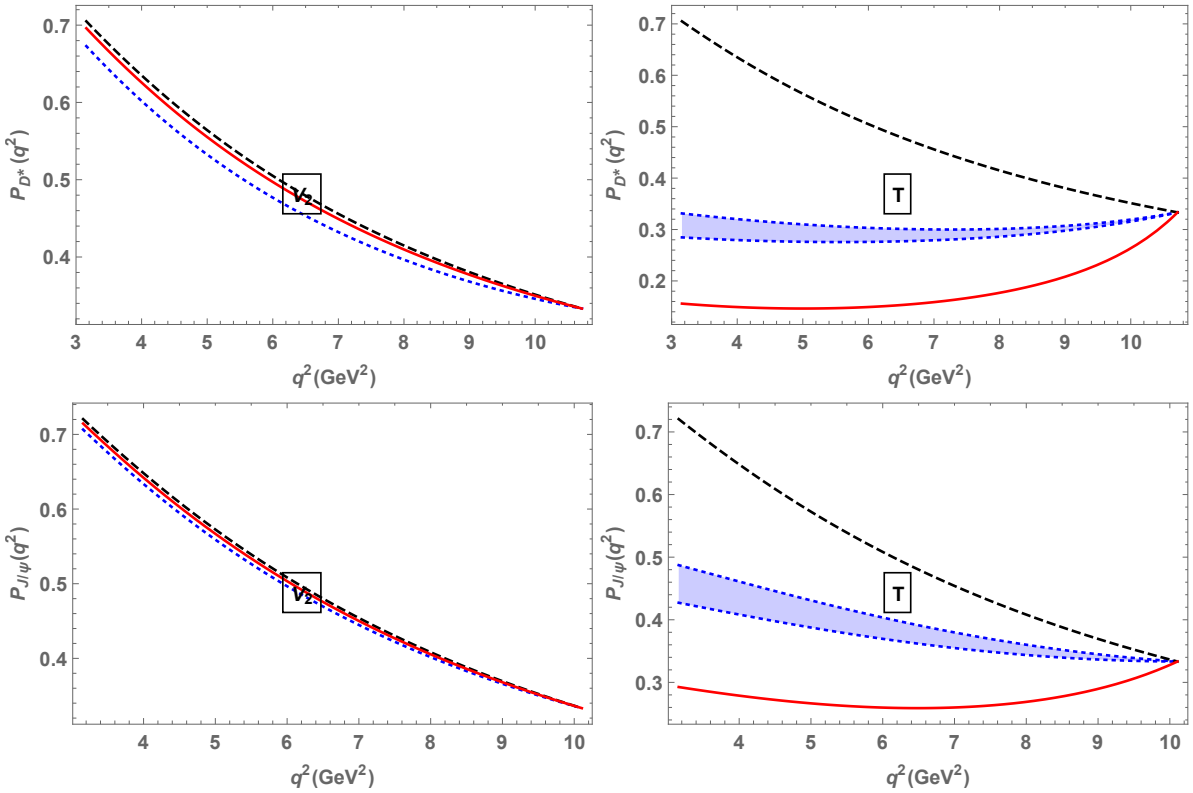

Figure: Predictions for the differential polarizations $P^{D^*}(q^2)$ and $P^{J/\psi}(q^2)$. The black dashed lines and the red solid lines respectively denote the SM predictions and the NP predictions corresponding to the best fitted Wilson coefficients. The light blue bands include NP effects corresponding to the experimental constraints within 2σ.

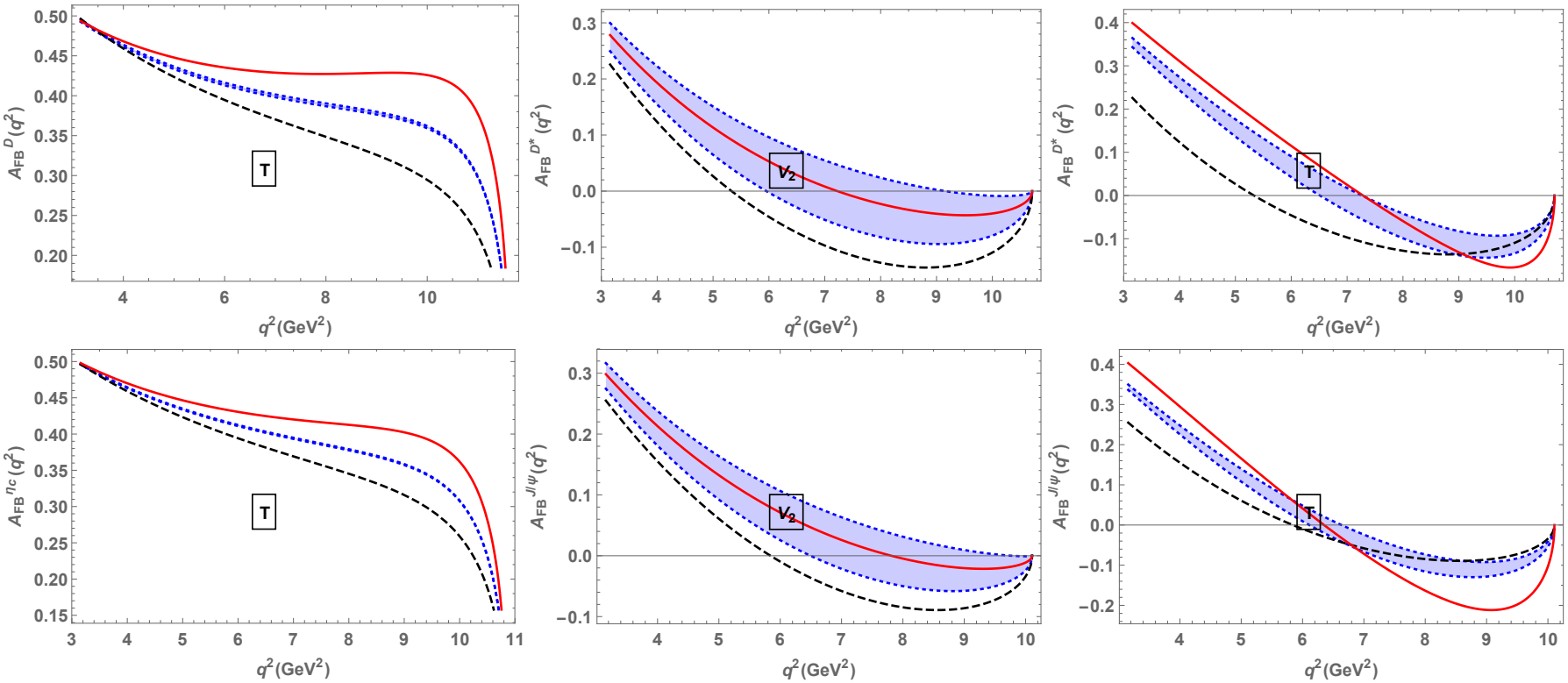

Figure: Predictions for the differential forward-backward asymmetries. The black dashed lines and the red solid lines respectively denote the SM predictions and the NP predictions corresponding to the best fitted Wilson coefficients. The light blue bands include NP effects corresponding to the experimental constraints within 2σ.

Summary and Conclusions

We have performed a model-independent analysis of the new physics effects in the $b \to c\tau\nu$ transitions within the framework of the effective field theory. Using the improved HQET form factors and CLFQM form factors, we find

- In the minimum χ^2 fit to the experimental measurements of $R(D^{(*)})$, $R(J/\psi)$ and $P_\tau(D^*)$, the V_2 scenario gives the smallest χ^2 value among the allowed scenarios.
- None of the single operators can explain simultaneously the current experimental measurements of the ratios $R(D)$, $R(D^*)$ and $R(J/\psi)$ at the confidence level of 1σ.
- Allowed regions for the Wilson coefficients of the vector and tensor operators (severely constrained) are obtained from the experimental constraints within 2σ along with the limit $\mathcal{B}(B_c \to \tau\nu) < 10\%$ from the LEP1 data.

- Our results suggest that any NP model dominated by a single scalar or tensor operator is under challenge, such as some types of charged Higgs models.
- The $R(D^*)$ anomalies have been amplified given our SM predictions, while the predicted $R(D)$ and $R(D^*)$ in the V_2 scenario are in excellent agreement with the current world average values.
- We have made predictions using the constraints on various physical observables for the $B \to D^{(*)}\tau\nu$ and $B_c \to \eta_c(J/\psi)\tau\nu$ decays, namely R, P_τ, P_M, and $\mathcal{A}_{FB}$, and the corresponding q^2 distributions.

Thank you!